On the Nature of Macroradicals Formed upon Radiolysis of Aqueous Poly(N-vinylpyrrolidone) Solutions

Clelia Dispenza,[1,2,] * Maria Antonietta Sabatino,[1] Natascia Grimaldi,[1,#] Björn Dahlgren,[3] Mohamad Al-Sheikhly,[4] James F. Wishart,[5] Zois Tsinas,[4] Dianne L. Poster,[6] and Mats Jonsson[3,*]

1. Dipartimento di Ingegneria, Università degli Studi di Palermo, Viale delle Scienze, 6, 90128 Palermo, Italy.
2. Istituto di BioFisica (IBF) – Consiglio Nazionale delle Ricerche, Via U. La Malfa, 153, 90146 Palermo, Italy.
3. Department of Chemistry, KTH Royal Institute of Technology, SE – 100 44 Stockholm, Sweden
4. Department of Materials Science and Engineering, University of Maryland, Maryland, USA
5. Chemistry Division, Brookhaven National Laboratory, Upton, NY 11973 USA
6. Materials Measurement Laboratory, National Institute of Standards and Technology (NIST), Gaithersburg, Maryland, USA

Abstract

In this work we have explored the nature of macroradicals formed upon radiolysis of aqueous poly(N-vinylpyrrolidone) (PVP) solutions using pulse radiolysis, density functional theory (DFT) and literature data. On the basis of literature data on site-specific kinetics of hydrogen abstraction from simple amides and spectra corresponding to specific radical sites on the same amides we have assessed the distribution of H-atom abstraction by •OH radicals from different positions on the pyrrolidone ring and the polymer backbone. Pulse radiolysis experiments performed at different doses per pulse and different PVP concentrations demonstrate that the H-abstracting radiolysis products are not quantitatively scavenged by the polymer when the dose per pulse exceeds ≈40 Gy. The implications of this are discussed in the context of radical-initiated crosslinking reactions. At a mass fraction of 0.1 % PVP and doses per pulse ranging from 7 Gy to 117 Gy, the overall radical decay observed at 390 nm follows second order kinetics with rate constants on the order of 10^9 $dm^3\ mol^{-1}\ s^{-1}$.

Keywords: poly(N-vinyl pyrrolidone), pulse radiolysis**,** density functional theory, macroradicals, nanogels.

Corresponding authors: Clelia Dispenza (clelia.dispenza@unipa.it)

Mats Jonsson (matsj@kth.se)

Current address:

Infinitec Activos, R&D Department, Barcelona Science Park, Helix Building, 15-21 Baldiri Reixac 08028 Barcelona, Spain.

Introduction

In these last two decades, nanogels have been developed for various applications including the *in vivo* transport or delivery of medical therapeutics (Oh et al., 2008; Kabanov and Vinogradov, 2009; Du et al., 2010; Ramos et al., 2014; Soni et al., 2016), separations of chemical or biological species (Luo et al., 2015; Kondo et al., 2010), catalysis (Resmini et al., 2012), sensor platforms (Reese et al., 2004, Wu and Zhou, 2010; Le Goff et al. 2015) and scaffolds for tissue or bone regeneration. (Sáez-Martínez et al., 2010; Molinos et al. 2012) The radiation-induced synthesis of nanogels from dilute aqueous polymer solutions using gamma (γ) or electron beam (e-beam) irradiation has been used extensively to successfully yield products that are well-tailored for these applications. (Dispenza et al., 2012a; Abd El-Rehim et al., 2013; Dispenza et al., 2014; Rashed et al., 2015; Adamo et al., 2016; Picone et al., 2016; Dispenza et al., 2017; Picone et al., 2018)

This approach takes advantage of the recombinant crosslinking reactions of radiolytically-produced free radicals on the polymer molecules to form the products. In particular, nanogel synthesis relies on intramolecular combination of radicals formed on the same polymer chain. Commonly used polymers are poly(N-vinylpyrrolidone) (PVP) (Ulanski and Rosiak, 1999; An et al., 2011; Dispenza et al., 2012b; Sabatino et al., 2013; Kadlubowski, 2014), poly(ethylene oxide) (PEO) (Ulanski et al. 1995), poly(vinyl alcohol) (Ulanski et al. 1998), poly(vinyl methyl ether) (Arndt et al. 2001; Querner et al.,2004; Schmidt et al., 2005), poly(N-

isopropyl acrylamide) (Picos-Corrales et al.,2012), polyacrylamide (El-Rehim, 2005), poly(acrylic acid) (PAA) (Ulanski et al., 2002; Kadlubowski et al., 2003), combinations of the above polymers (Henke et al. 2005, Ghaffarlou et al., 2018), and PVP in the presence of small quantities of acrylic monomers. (Dispenza et al., 2012a; Grimaldi et al., 2014)

Chemical reactions initiated by ionizing radiation in dilute aqueous solutions are predominantly associated with the radiolysis of water, producing reactive radical species and molecular products (e_{aq}^-, $^{\bullet}OH$, H, H_2, H_2O_2 and H_3O^+). They cover a broad range of reactivities, with both strong oxidants (*e.g.,* $^{\bullet}OH$, the hydroxyl radical) and reductants (*e.g.,* e_{aq}^-, the aqueous electron, historically referred to as the hydrated electron). The radiation chemical yields of $^{\bullet}OH$ and e_{aq}^- in Ar-saturated solutions are $G(^{\bullet}OH) = 2.8 \times 10^{-7}$ mol J^{-1}, and $G(e_{aq}^-) = 2.8 \times 10^{-7}$ mol J^{-1}. All the other species have significantly lower G-values. (Spinks and Woods, 1990) By saturating the aqueous solutions with N_2O prior to irradiation, e_{aq}^- is converted to $^{\bullet}OH$ through reaction (1),

$$e_{aq}^- + N_2O \rightarrow N_2 + O^{\cdot -} \xrightarrow{H_2O} N_2 + {}^{\cdot}OH + OH^- \qquad k = 9.1 \times 10^9 \text{ dm}^3 \text{ mol}^{-1} \qquad (1)$$

which effectively doubles the yield of $^{\bullet}OH$ to 5.6×10^{-7} mol J^{-1}. (Spinks and Woods, 1990)

Radicals and molecular products are homogeneously distributed in the bulk liquid of the system after about 10^{-7} seconds and subsequently react with the solute, inducing the formation of secondary radiolysis products. The radiolytically produced $^{\bullet}OH$ radicals react rapidly with polymer chains through hydrogen abstraction (reaction (2)).

$$^{\cdot}OH + PVP \rightarrow H_2O + [PVP - H]^{\cdot} \qquad (2)$$

The general assumption is that all of the $^{\bullet}OH$ radicals react with the polymer, which would produce a stoichiometric number of carbon-centered polymer radicals. This assumption holds true for concentrated aqueous polymer solutions irradiated at a relatively low dose rate, i.e. by γ-irradiation. (Sakurada and Ikada, 1963; Hoffman and Allan, 1977; Rosiak et al., 2002; Dispenza et al. 2016a) In dilute or semi-dilute polymer solutions irradiated with an e-beam at high dose rates (high dose per pulse and/or high pulse frequency), the $^{\bullet}OH$ will not only abstract

hydrogen from the polymer, but will also react with itself (reaction (3)) with a high reaction rate constant (k = 5.5 x 10^9 dm^3 mol^{-1} (Buxton et al. 1988).

$$^{\cdot}OH + {}^{\cdot}OH \rightarrow H_2O_2 \quad (3)$$

From the competing reactions (2) and (3) follows that the efficiency of H-abstraction from PVP, and thereby the formation of carbon-centered polymer radicals, depends on the concentration of PVP and also on the transient concentration of •OH in the solution. When using pulsed e-beam irradiation, the transient concentration of •OH is governed by the dose rate. Higher dose rates yield higher transient •OH concentrations that require higher polymer concentrations to prevent •OH recombination. The non-quantitative H-abstraction in dilute aqueous solutions of polyethylene oxide (PEO) was demonstrated by pulse radiolysis experiments with spectrophotometric detection. (Ulanski et al. 1995) More recently, the same behavior was observed for e-beam irradiated PVP aqueous solutions through experimental quantification of hydrogen peroxide formation and predicted by numerical simulations of the radiation chemistry of the corresponding systems. (Dispenza et al., 2016b; Ditta et al., 2019)

For most polymers, there are several possible radical sites on each repeating unit. The H-abstraction sites and the resulting C-centered radicals formed upon reaction between •OH and PVP or structurally similar compounds have been discussed extensively, but there is limited experimental evidence to support the proposed free-radical intermediate structures. (Davis et al., 1981; Rosiak et al., 1990; An et al. 2011, Bartoszek et al. 2011) Work in the early 1970s by Taniguchi is often referred to in discussions regarding the nature of free-radical intermediates. (Taniguchi, 1970) Using electron spin resonance, Taniguchi demonstrated the production of free-radical intermediates from the reaction of •OH with nitrogen heterocyclic compounds and pyrimidine derivatives in acidic (pH 1.4-2.2) solutions containing Ti^{3+} and H_2O_2. (Taniguchi, 1970) He concluded that •OH abstracts the hydrogen atom preferentially from the C-H bond adjacent to the imino group or to the nitrogen atom of the heterocyclic ring. However, this conclusion is not based on studies of N-substituted pyrrolidones or on PVP. Taniguchi stresses that N-methyl-2-pyrrolidone and N-vinyl-2-pyrrolidone did not give any resolved Electron Paramagnetic Resonance spectra of their

intermediate radicals and noted that nitroxide radicals from pyrrolidine were not observed. (Taniguchi, 1970) In 1971, Hayon and colleagues (Hayon et al., 1971) studied the sites of •OH abstraction from linear N-alkylated amides in aqueous solutions using pulse radiolysis. According to their study, the rate constant for hydrogen abstraction from an alkyl C-H adjacent to the amide nitrogen of N-alkyl amides was shown to be significantly higher than the value for hydrogen abstraction from the CH_2-group adjacent to the carbonyl group. Their work includes kinetic data and spectral information for the different radical structures that may possibly be formed upon hydrogen abstraction from N-alkyl amides.

To further explore the nature of PVP-radicals produced upon radiolysis and the efficiency in converting •OH into macroradicals in dilute solutions, we used pulse radiolysis transient absorption spectroscopy over the wavelength range of 350 nm to 500 nm (at 10 nm intervals) to obtain the transient spectra of irradiated aqueous PVP. DFT was also applied to interrogate the stability and spectral properties of the different possible radicals that form on the pyrrolidone ring upon reaction between •OH and PVP. The predicted spectral features of the various radicals were compared with the experimental transient spectra of irradiated aqueous PVP. Our experimental results are discussed in view of the previously published data. In addition, we conducted and analyzed a series of pulse radiolysis experiments on aqueous solutions of PVP at different concentrations and doses per pulse.

Experimental

Materials

Poly(N-vinyl pyrrolidone) (PVP K60, average M_w 0.46 MDa) was supplied by Sigma-Aldrich (Italy) as aqueous solution at 45 % mass fraction.

DFT calculations

The computed spectra of the various radicals were obtained from time-dependent DFT calculations using the Gaussian 09 program suite. (Frisch et al., 2010) Geometry optimizations using DFT were performed at the B3LYP/6-31G(d) level of theory. The spectra were then calculated using time-dependent DFT at the CAM-

B3LYP/6-311+G(2d,p) level of theory. To test if solvation plays a dominant role in determining the reactivity of different sites toward H-abstraction, analogous computations (geometry optimization followed by a TDDFT calculation) were performed using the Polarizable Continuum Model (PCM) with the permittivity of water. The impact of including an explicit number of water molecules (up to 3) was also investigated, although this was found to have little effect. To see which radicals were most stable, we compared the relative electronic energies amongst each other, noting the variance in the energy between the different structures increased as the number of water molecules considered was increased. Therefore, we took the relative energies as the average between the four cases when considering one explicit water molecule with or without implicit solvation. The standard deviation from this pool of 4 values serves as an indication of the error with respect to solvation model, i.e., PCM. We also investigated the impact of using another functional theory (M06-2X). We concluded that it had little impact on the energies (the difference was less than 1 kJ/mol) and negligible difference on the calculated electronic spectra.

Pulse radiolysis

Electron pulse-radiolysis transient-absorption experiments were performed on the 2 MeV Van de Graaff accelerator at Brookhaven National Laboratory using a PC-based data acquisition and control system. Diluted PVP solutions at (0.05±0.01) % mass fraction, (0.10±0.01) % mass fraction, (0.25±0.01) % mass fraction and (0.50±0.01) % mass fraction were prepared by adding deionized water ($\rho \geq 18.2$ MΩ cm) and saturated with N_2O prior to irradiation. The uncertainty represents the estimated total error in measuring mass and volume of solutions. The irradiation was performed in a rectangular quartz cell 20 mm x 10 mm x 5 mm and re-filled between each experiment. The e-beam (*xy* dimension) was directed through the 5-mm-thick axis of the cell, and the optical axis for the transient absorbance measurements passed through the 20 mm path length, at a right angle to the e-beam. The standard deviation of the absorbance measurements was 0.001 AU. Irradiated solutions were drained from the cell after use, so the solution in the reservoir remained fresh until it was used. The sample temperature was regulated at 25.0 ˚C. Pulse widths of 0.2 μs, 1.0 μs and 5.0 μs were

used to deliver doses of 7 Gy per pulse, 40 Gy per pulse and 117 Gy per pulse, respectively. Dosimetry was performed using an aqueous, N_2O-saturated, 10 mmol KSCN solution and measuring the absorbance at 472 nm assuming that the yield and extinction coefficient of the $(SCN)_2^{\bullet-}$ radical anion are G = 0.64 μmol J^{-1} absorbed and ε_{472} = 7950 $dm^3\,mol^{-1}\,cm^{-1}$, respectively.

The data were fit with simplified integrated rate equations assuming that the reaction kinetics are either first order in free radical concentration ($R^{\cdot} = R_0^{\cdot} e^{-kt}$) or second order in free radical concentration ($R^{\cdot} = R_0^{\cdot}/[1 + ktR_0^{\cdot}]$), where $R^{\cdot}$ is the time-resolved concentration of free radicals, $R_0^{\cdot}$ is the concentration at t = 0 and k is the rate constant. Weighed fits were performed with the Levenberg-Marquardt fitting algorithm for each model using the Igor Pro software package (Wavemetrics, Portland, OR).

Results and Discussion

Spectral properties of radical intermediates formed in pulse radiolysis of aqueous PVP solutions.

In N_2O saturated 0.25 % mass fraction PVP aqueous solution, the transient spectra of the PVP radicals were measured by pulse radiolysis at 10 nm intervals over the wavelength range of 350 nm to 500 nm. The resulting initial spectra obtained directly after the pulse with a width of 5.0 microseconds (t = 5.0 μs) is shown in Figure 1 along with the spectrum at t = 800 μs after the pulse.

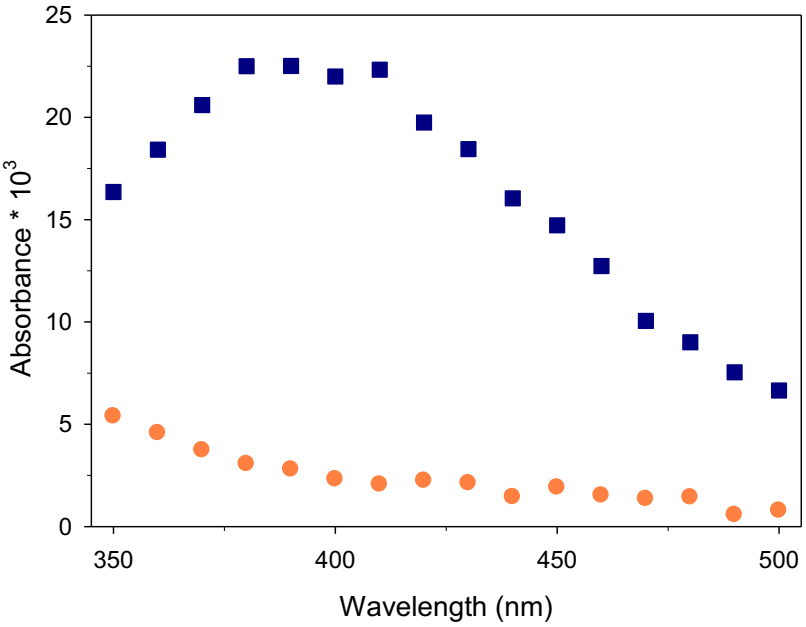

Figure 1. Absorbance spectra immediately after the 5 μs pulse (blue squares); and 800 μs after the pulse (orange circles); PVP concentration equal to 0.25 % mass fraction in deionized H_2O. Standard deviation in the absorbance measurement is 0.001 AU.

The initial transient spectrum displays a broad peak with a maximum at ≈390 nm indicating the presence of PVP free radicals (Figure 1). This is in good agreement with previous pulse radiolysis studies on this polymer. (Davis et al., 1981; An et al., 2011) The transient spectrum at 800 μs after the pulse no longer shows the feature at 390 nm and the residual absorbance at 350 nm suggests the presence of species with absorption peaks at shorter wavelengths. The molar absorptivity for the PVP-radicals at 390 nm was calculated from the initial absorbance at the lowest dose per pulse (7 Gy) and the highest polymer mass fraction (0.5 %), because these conditions ensure quantitative conversion of the primary radiolysis products into PVP-radicals (see below). The resulting molar absorptivity assuming that both hydroxyl radicals and hydrogen atoms yield PVP-radicals is ε_{390} = 670 $dm^3\ mol^{-1}\ cm^{-1}$.

To further explore the spectral properties of PVP-based radicals, we performed DFT calculations on the different radical structures illustrated in Figure 2. Table 1

summarizes the predicted relative energy (corresponding to the relative C-H bond dissociation enthalpy of the parent compound) and the wavelength of the maximum absorbance obtained for each structure. We can expect •OH to abstract also the beta-hydrogen from the backbone. The corresponding radical (not shown in Figure 2) will most probably have similar relative energy and peak absorbance wavelength to Radical 2.

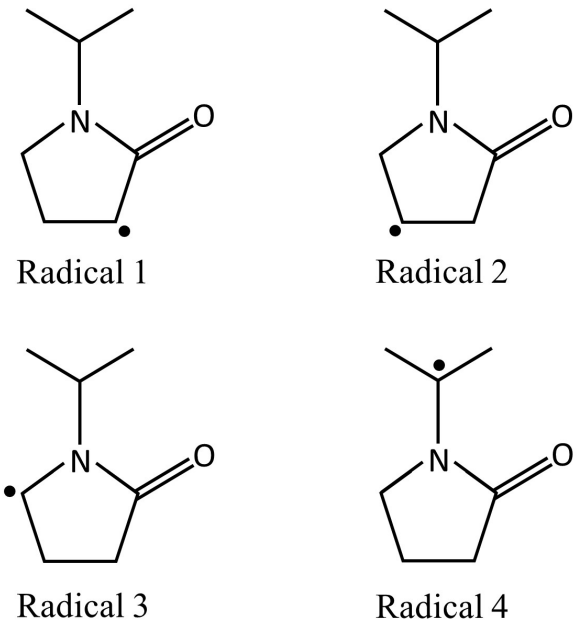

Figure 2. Molecular structures of four radicals studied using DFT calculations

Table 1. Predicted relative energies, and peak absorbance wavelengths from DFT calculations for the radicals depicted in Figure 2.

Radical	Relative energy (kJ mol^{-1})	λ_{max} (nm)	Distribution of radicals(1)
1	8 ±4	424	14 %
2	23 ±2	252	8.5 %
3	0	327	46 %
4	9 ±2	323	23 %

(1) calculated using relative rate constant data presented in Hayon et al., 1971.

From the predicted values of λ_{max} of Table 1, the initial transient spectrum shown in Figure 1 can be mainly attributed to Radicals 1, 3 and 4 shown in Figure 2. These results are in good agreement with literature data from Davis et al. 1981 on the absorption spectra of the transient species formed when pulsing aqueous solutions of saturated pyrrolidone derivatives, such as pyrrolidone, N-methylpyrrolidone, N-ethylpyrrolidone and 1,1-bis(2-oxopyrrolidin-1-yl)ethane). (Davis et al., 1981) Indeed, all the spectra are similar, suggesting that water radiolysis products react mainly at the pyrrolidone ring or that only radicals formed on the ring contribute to the absorbance in this wavelength range (i.e. other radicals formed may not be visible).

The rate constant for hydrogen abstraction from the alfa-position on the backbone leading to Radical 4, measured on structurally analogous, low molecular weight compounds, is of the order of 2 x 10^9 dm^3 $mol^{-1}s^{-1}$. (Davis et al., 1981) Caution is advisable in transferring this information to the rate constant for Radical 4 formation on the polymer. Davies et al. have demonstrated that the reaction of •OH radical with PVP is one order of magnitude lower (≈2 x 10^8 dm^3 mol^{-1} s^{-1}) than that for its reaction with the low molecular weight saturated pyrrolidones. (Davis et al., 1981) Moreover, Behzadi et al. 1970 have shown that for diluted PVP solutions, the rate constant decreases with increasing degree of polymerization. (Behzadi et al., 1970) More recent studies of Bartoszek et al. 2011 have also shown a decrease in the overall rate constant of the reactions between •OH and PVP with increasing the molecular weight of the polymer. (Bartoszek et al. 2011) Even though the absolute rate constants for the polymer and a low molecular weight analogue of its repeating unit may be different, the relative rate constants for hydrogen abstraction from different positions can be assumed to be the same, unless steric hindrance limits specific sites accessibility. Considering that PVP in water at low concentration is reported to have a random coil conformation (Kadlubowski S. 2014), we expect steric hindrance to affect all sites equally.

The already-mentioned study of Hayon et al. 1971 provides the rate constants for hydrogen abstraction by •OH from different positions of N-alkylated amides. (Hayon et al., 1971) The rate constants per H-atom are the following: 1.6 x 10^8 dm^3

mol^{-1} s^{-1} for α–C-H, 1.0 x 10^8 dm^3 mol^{-1} s^{-1} for β–C-H and 5.5 x 10^8 dm^3 mol^{-1} s^{-1} for C-H adjacent to the nitrogen. These rate constants were used to estimate the relative distribution among the possible radical structures depicted in Figure 2, as reported in Table 1. Judging from the kinetic analysis, the predominant radical structure is Radical 3. This is in agreement with the relative energy predicted by the DFT calculations and with the observations made by Taniguchi. (Taniguchi 1970) Radicals 4 and 1 contribute by 23 % and 14 % to the distribution, again in qualitative agreement with DFT calculations. The secondary radical of the ring (Radical 2), similarly to the secondary radical of the polymer backbone, contribute by 8.5 % each to the distribution. This implies that hydrogen abstraction from PVP by the hydroxyl radical is not stochastic but rather displays some selectivity that appears to be governed by the relative C-H bond dissociation energies. On the basis of the relative distribution of the radicals and their respective molar extinction coefficients, given by Hayon et al. 1971, we can estimate the relative contribution of the radicals to the spectrum. The relative contributions to the spectrum are 12 % for Radical 1, 59 % for Radical 3, and 29 % for Radical 4.

To investigate the scavenging capacity of the system, single-pulse experiments were performed on polymer solutions with concentrations ranging from 0.05 % mass fraction to 0.5 % mass fraction at three different doses per pulse. The initial absorbance at 390 nm increases with the dose per pulse at every polymer concentration (Table 2). Moreover, the initial absorbance also increases with polymer concentration at the two higher doses per pulse. This is clearly evident in Figure 3, where the relative initial absorbance with respect to the lowest polymer concentration as function of PVP concentration for the various doses per pulse is presented. The polymer concentration dependence observed for 40 Gy per pulse and 117 Gy per pulse shows that we do not have quantitative conversion of •OH to PVP-based radicals under those two irradiation conditions, hence reaction (3) starts to effectively compete with reaction (2). These findings are in very good agreement with a recently published study on numerical simulations of the kinetics of macroradical decay in electron pulse irradiated dilute polymer solutions (Dahlgren et al., 2019). Moreover, the insufficient scavenging capacity of the polymer at low concentrations for the transiently formed •OH leads to

recombination of the latter, yielding H_2O_2 and subsequently also O_2. Evidence of H_2O_2 and O_2 formation in initially deoxygenated solutions has been experimentally confirmed by quantitative detection of H_2O_2 in irradiated aqueous PVP systems (Ditta et al. 2019) and by several spectroscopic characterizations carried out on the irradiated polymer, revealing the presence of 5-members cyclic imides, carboxyl groups and C-O-C crosslinks (Sabatino at al. 2013).

Table 2. Absorbance immediately after the pulse for various mass fractions of PVP and doses per pulse

Dose per pulse (Gy)	Initial absorbance[a]			
	0.05 %	0.10 %	0.25 %	0.50 %
7	0.006	0.006	0.006	0.006
40	0.018	0.020	0.024	0.028
117	0.072	0.090	0.110	0.150

[a] Standard Deviation = 0.001 AU

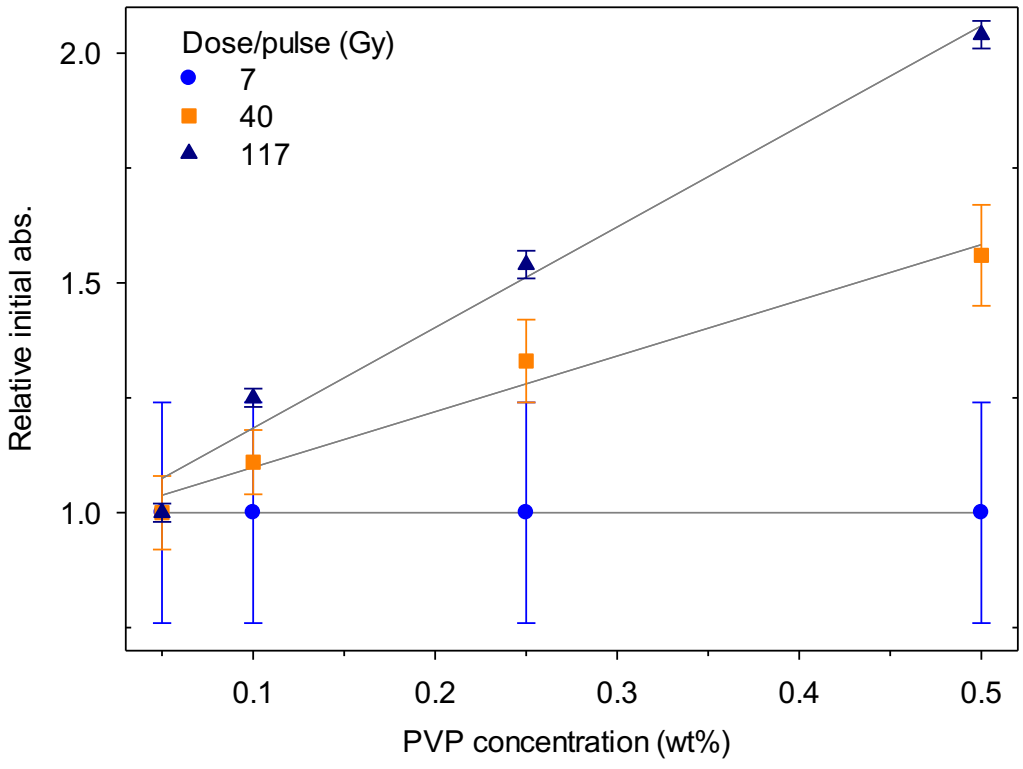

Figure 3. Relative initial absorbance (with respect to the lowest polymer concentration) as a function of PVP concentration for three different doses per pulse. Error bars account for 1 standard deviation in the absolute absorbances.

Kinetics of PVP-radical decay

Analysis of the kinetics of macroradical decay in solution is not straightforward. For most commercial polymers, the molecular weight distribution is fairly broad and this surely influences the kinetics. The possibility of having multiple radical sites on the same macromolecule also enables intramolecular radical-radical reactions to compete with the intermolecular radical-radical reactions. As a consequence, macroradical decay in solution is often described using dispersive kinetics instead of the more conventional second order kinetics that can be expected for bimolecular reactions (Jeszka et al. 2006). The competition with intramolecular radical-radical reactions is handled with the recourse to a time dependent overall rate constant accounting for all the processes consuming macroradicals in the system. It is interesting to note that recent modeling efforts have been shown to be able to handle the competition between intra- and intermolecular reactions and molecular size dependence using classical second order kinetics (Dahlgren et al. 2019, Dahlgren et al. 2020).

The kinetics of the PVP-radical decay were investigated by monitoring the absorbance at 390 nm at doses per pulse of 40 Gy and 117 Gy. The time-resolved absorbance plots for 0.1 % mass fraction PVP and relative second-order decay fits are shown in Figure 4. Indeed, the reduced χ^2 values were smaller for the second order model than the first order model and no systematic deviation can be observed. Hence, second-order kinetics appears to describe the radical decay in this study sufficiently well. The resulting rate constant for a dose per pulse of 117 Gy is (2.1±0.1) x 10^9 dm^3 mol^{-1} s^{-1}. This value agrees fairly well with previously published work by An et al. 2011, where the second-order decay rate constant of PVP-radicals at room temperature was reported to be 1.1 x 10^9 dm^3 mol^{-1} s^{-1}. (An et al., 2011) The reaction rate constant at 40 Gy per pulse did not change appreciably, the resulting value being (3.4±0.1) x 10^9 dm^3 mol^{-1} s^{-1}. The slight difference in second-order rate constant between the two doses per pulse may be

a consequence of the different number of radicals per macromolecule in the two cases. The second order decay kinetics of 7 Gy per pulse is not shown here because the signal-to-noise ratio of the absorbance data obtained was high and the data could not be processed with confidence.

a)

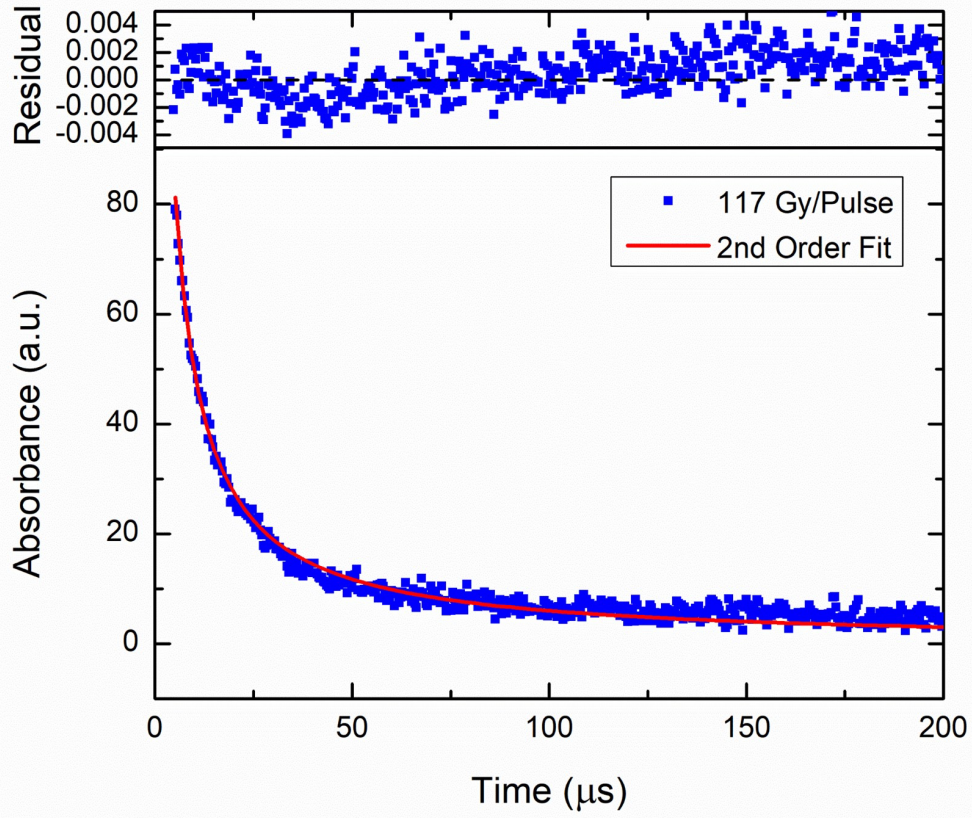
Residual
0.004
0.002
0.000
-0.002
-0.004
Absorbance (a.u.)
80
60
40
20
0
117 Gy/Pulse
2nd Order Fit
0
50
100
150
200
Time (μs)

b)

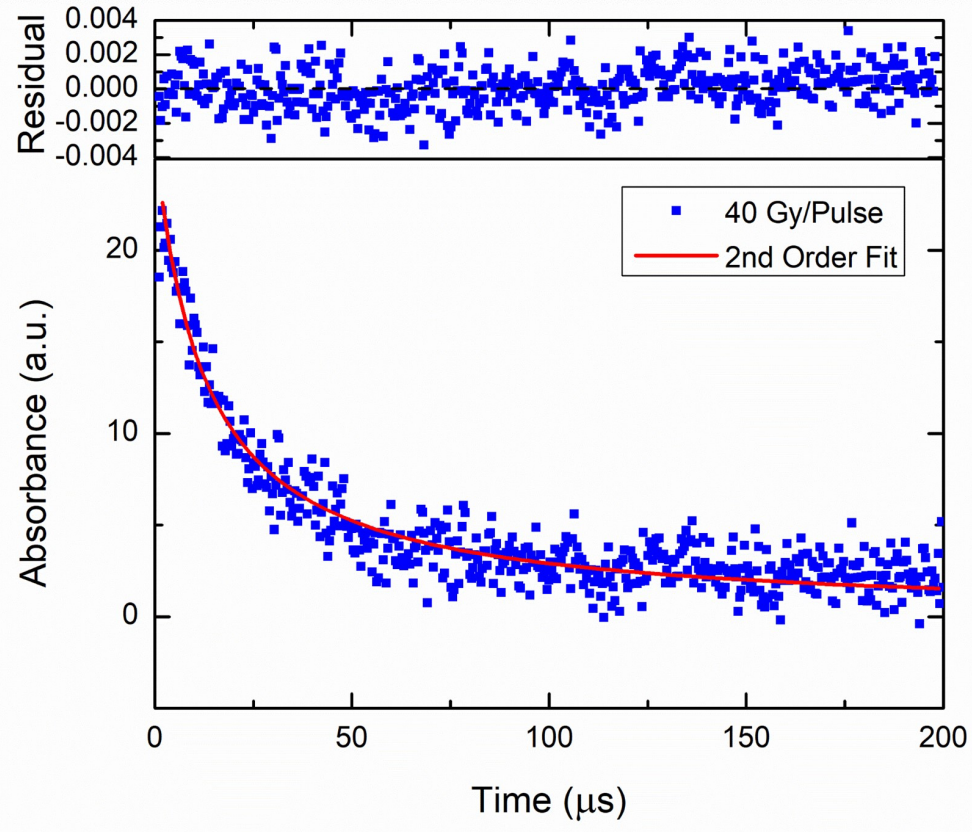
Residual
0.004
0.002
0.000
-0.002
-0.004
Absorbance (a.u.)
20
10
0
40 Gy/Pulse
2nd Order Fit
0
50
100
150
200
Time (μs)

Figure 4. Decay kinetics of [PVP-H]• at 390 nm and fit residuals; pulse radiolysis of N_2O-saturated 0.1% mass fraction PVP solutions measured at 25 °C and doses of: a) 117 Gy per pulse, and b) 40 Gy per pulse.

Conclusions

Based on literature data with the qualitative support of DFT calculations performed in this work, it has been concluded that the visible spectrum of the PVP-radicals produced by H-abstraction from the •OH radicals results from the contribution of three principal radicals that constitute more than 80 % of the total amount of the PVP radical species formed. Pulse radiolysis experiments indicate that the conversion of radicals from water radiolysis is quantitative only at the lowest dose per pulse used in this study. In contrast, for the higher doses per pulse, a polymer concentration dependence on the maximum absorbance after the pulse is observed. Since the PVP solutions used in this study are dilute, at the higher doses per pulse, the •OH radical self-reaction competes with the •OH radical reaction with the polymer, decreasing the yield of polymer radicals. The overall second-order decay rate constant of the formed PVP-radicals is on the order of 2 $x10^9$ dm^3 mol^{-1} s^{-1} to 3 $x10^9$ dm^3 mol^{-1} s^{-1}, which is slightly higher than the previously reported value of 1 $x10^9$ dm^3 mol^{-1} s^{-1}. This is due to the use of a slightly higher molar extension coefficient in the previous work.

Acknowledgments

The work at BNL and use of the 2 MeV electron Van de Graaff of the BNL Accelerator Center for Energy Research were supported by the US Department of Energy, Office of Basic Energy Sciences, Division of Chemical Sciences, Geosciences, and Biosciences under contract # DE-SC0012704.

DLP thanks Dr. John J. Kasianowicz, senior biophysicist of the Microsystems and Nanotechnology Division of the Physical Measurement Laboratory for helpful discussions on the manuscript.

CD acknowledges the support of the University of Palermo, Fondo Finalizzato per la Ricerca (FFR 2018/2021).

Certain commercial materials, equipment and instruments may be identified in this work to describe the experiments as completely as possible. In no case does such identification imply a recommendation of endorsement by the National Institute of Standards and Technology, nor does it imply that the materials, equipment or instruments identified are necessarily the best available for the purpose.

REFERENCES

Adamo, G., Grimaldi, N., Campora, S., Bulone, D., Bondì, M.L., Al-Sheikhly, M., et al., 2016. Multi-functional nanogels for tumor targeting and redox-sensitive drug and siRNA delivery. Molecules 21(11), E1594-1612.

An, J.C., Weaver, A., Kim, B., Barkatt, A., Poster, D., Vreeland, W.N., et al., 2011. Radiation-induced synthesis of poly(vinylpyrrolidone) nanogel. Polymer 52, 5746–5755.

Arndt, K.F., Schmidt, T., Reichelt, R., 2001. Thermo-sensitive poly(methyl vinyl ether) micro-gel formed by high energy radiation. Polymer 42, 6785–6791.

Bartoszek, N., Ulanski, P., Rosiak, J.M. 2011. Reaction of a low-molecular-weight free radical with a flexible polymer chain: Kinetic studies on the OH + poly(N-vinylpyrrolidone model. Int. J. Chem. Kinet., 43 (9), 474-481.

Behzadi, A., Borgwardt, U., Henglein, A., Schamberg, E., Schnabel, W., 1970. Pulsradiolytische untersuchung der kinetik diffusionskontrollierter reaktionen des OH-radikals mit polymeren und oligomeren in wäßriger lösung bunsenges. Phys. Chem. 74(7), 649-653.

Buxton, G.V., Greenstock, C.L., Helman, W.P., Ross, A.B., 1988. Critical-Review of Rate Constants for Reactions of Hydrated Electrons, Hydrogen-Atoms and Hydroxyl Radicals(•OH/•O−) in Aqueous-Solution. J. Phys. Chem. Rev. Data 17, 513–886.

Dahlgren, B., Dispenza, C., Jonsson, M., 2019. Numerical simulation of the kinetics of radical decay in single-pulse high-energy electron-irradiated polymer aqueous solutions. J. Phys. Chem. A 123, 5043-5050.

Dahlgren, B., Sabatino, M. A., Dispenza, C., Jonsson, M., 2020. Numerical simulations of nanogel synthesis using pulsed electron beam. Macromol. Theory Simul. 29, 1900046-58.

Davis, J.E., Sangster, D.F., Senogles, E., 1981. Pulse Radiolysis of Aqueous Solutions of N-Vinylpyrrolidin-2-one and Poly(N-vinylpyrrolidin-2-one). Aust. J. Chem. 34, 1423-1431.

Dispenza, C., Sabatino, M.A., Grimaldi, N., Bulone, D., Bondì, M.L., Casaletto, M.P., et al., 2012a. Minimalism in radiation synthesis of biomedical functional nanogels. Biomacromolecules 13, 1805-1817.

Dispenza, C., Sabatino, M.A., Grimaldi, N., Spadaro, G., Bulone, D., Bondì, M.L., et al., 2012b. Large-scale radiation manufacturing of hierarchically assembled nanogels. Chem. Eng. Trans. 27, 229C–234C.

Dispenza, C., Adamo, G., Sabatino, M.A., Grimaldi, N., Bulone, D., Bondì, M.L., et al., 2014. Oligonucleotides-decorated-poly(N-vinyl pyrrolidone) nanogels for gene delivery. J. Appl. Polym. Sci. 131, 39974-82.

Dispenza, C., Spadaro, G., Jonsson, M., 2016a. Radiation engineering of multifunctional nanogels. Top. Curr. Chem. 374(5), 69-95.

Dispenza, C., Sabatino, M.A., Grimaldi, N., Mangione, M.R., Walo, M., Murugan, E. et al., 2016b. On the origin of functionalization in one-pot radiation synthesis of nanogels from aqueous polymer solutions, RSC Adv. 6, 2582-2591.

Dispenza, C., Sabatino, M.A., Ajovalasit, A., Ditta, L.A., Ragusa, M., Purrello, M., et al., 2017. Nanogel-antimiR-31 conjugates affect colon cancer cells behaviour. RSC Adv. 7, 52039.

Ditta, L.A., Dahlgren, B., Sabatino, M.A., Dispenza, C., Jonsson, M., 2019. The role of molecular oxygen in the formation of radiation-engineered multifunctional nanogels. Eur. Polym. J. 114, 164-175.

Du, J.-Z., Sun, T.-M., Song, W.-J., Wu, J., Wang, J., 2010. Tumor-acidity-activated charge-conversional nanogel as an intelligent vehicle for promoted tumoral-cell uptake and drug delivery. Angew. Chem. Int. Ed. 49, 3621–3626.

El-Rehim, H.A.A., 2005. Swelling of radiation crosslinked acrylamide-based microgels and their potential applications. Radiat. Phys. Chem. 74(2), 111–117.

El-Rehim, H.A.A., Swilem, A.E., Klingner, A., Hegazy, E.-S.A., Hamed, A.A., 2013. Developing the potential ophthalmic applications of pilocarpine entrapped into polyvinylpyrrolidone-poly(acrylic acid) nanogel dispersions prepared by γ radiation. Biomacromolecules 14(3), 688-698.

Frisch, M.J., Trucks, G.W., Schlegel, H.B., Scuseria, G.E., Robb, M.A., et al., 2010. Gaussian 09, Revision C.01, Gaussian Inc., Wallingford CT.

Ghaffarlou, M., Duygu Sütekin, S., Güven, O., 2018. Preparation of nanogels by radiation-induced cross-linking of interpolymer complexes of poly (acrylic acid) with poly (vinyl pyrrolidone) in aqueous medium. Radiat. Phys. Chem. 142, 130–136.

Grimaldi, N., Sabatino, M.A., Przybytniak, G., Kaluska, I., Bondì, M.L., Bulone, D., et al., 2014. High-energy radiation processing, a smart approach to obtain PVP-graft-AA nanogels. Radiat. Phys. Chem. 94, 76–79.

Hayon, E., Ibata, T., Lichtin, N.N., Simic, M., 1971. Sites of attack of hydroxyl radicals on amides in aqueous solution. II. Effects of branching, α to carbonyl and to nitrogen. J. Am. Chem. Soc. 93, 5388-5394.

Henke, A., Kadlubowski, S., Ulanski P, Rosiak J.M., Arndt 2005. Radiation-induced crosslinking of polyvinylpyrrolidone-poly(acrylic acid) complexes. Nucl. Instrum. Methods Phys. Res. B. 236, 391-398.

Hoffman, A.S., Allan, S., 1977. A review of the use radiation plus chemical and biochemical processing treatments to prepare novel biomaterials. Radiat. Phys. Chem. 18(1-2), 323-342.

Jeszka, J. K., Kadlubowski, S., Ulanski, P., 2006. Monte Carlo simulations of nanogels formation by intramolecular recombination of radicals on polymer chain. Dispersive kinetics controlled by chain dynamics. Macromolecules 39, 857-870.

Kabanov, A.V., Vinogradov, S.V., 2009. Nanogels as pharmaceutical carriers: Finite networks of infinite capabilities. Angew. Chem. Int. Ed. 48, 5418–5429.

Kadlubowski, S., Grobelny, J., Olejniczak, W., Cichomski, M., Ulanski, P., 2003. Pulses of fast electrons as a tool to synthesize poly(acrylic acid) nanogels.

Intramolecular cross-linking of linear polymer chains in additive-free aqueous solution. Macromolecules 36(7), 2484–2492.

Kadlubowski, S., 2014. Radiation-induced synthesis of nanogels based on poly(N-vinyl-2-pyrrolidone)—A review. Radiat. Phys. Chem. 102, 29–39.

Kondo, K., Kaji, N., Toita, S., Okamoto, Y., Tokeshi, M., Akiyosh,i K., et al. 2010. DNA separation by cholesterol-bearing pullulan nanogels. Biomicrofluidics 4(3), 32210–32218.

Le Goff, G.C., Srinivas, R.L., Hill, W.A., Doyle, P.S., 2015. Hydrogel microparticles for biosensing. Europ. Polym. J. 72, 386–412.

Luo, F., Xie, R., Liu, Z., Ju, X.-J., Wang, W., Lin, S., et al., 2015. Smart gating membranes with in situ self-assembled responsive nanogels as functional gates. Sci. Rep. 5, 14708–14721.

Molinos, M., Carvalho, V., Silva, D.M., Gama, F.M., 2012. Development of a hybrid dextrin hydrogel encapsulating dextrin nanogel as protein delivery system. Biomacromolecules 13, 2517-2527.

Oh, J.K., Drumright, R., Siegwart, D.J., Matyjaszewski, K., 2008. The development of microgels/nanogels for drug delivery applications. Prog. Polym. Sci. 33, 448–477.

Picone, P., Ditta, L.A., Sabatino, M.A., Militello, V., San Biagio, P.L., Di Giacinto, M.L., et al., 2016. Ionizing radiation-engineered nanogels as insulin nanocarriers for the development of a new strategy for the treatment of Alzheimer's disease. Biomaterials 80, 179–194.

Picone, P., Sabatino, M.A., Ditta, L.A., Amato, A., San Biagio, P.L., Mulè, F., et al., 2018. Nose-to-brain delivery of insulin enhanced by a nanogel carrier. J. Control. Release 270, 23–36.

Picos-Corrales, L.A., Licea-Claverìe, A., Arndt, K.-F., 2012. Stimuli-responsive nanogels by e-beam irradiation of dilute aqueous micellar solutions: Nanogels with pH controlled LCST. Chapter 7: Polymer Nanotechnology. In: Nanotechnology: advanced materials, CNTs, particles, films and composites, Technical Proceedings, Vol 1. Tech Connect/CRC Press/NSTI joint publication. Pp 644-647.

Querner, C., Schmidt, T., Arndt, K.F., 2004. Characterization of structural changes of poly(vinyl methyl ether) gamma-irradiated in diluted aqueous solutions. Langmuir 20(7), 2883–2889.

Ramos, J., Forcada, J., Hidalgo-Alvarez, R., 2014. Cationic polymer nanoparticles and nanogels: From synthesis to biotechnological applications. Chem. Rev. 114, 367–428.

Rashed, E.R., Abd El-Rehim, H.A., El-Ghazaly, M.A., 2015. Potential efficacy of dopamine loaded-PVP/PAA nanogel inexperimental models of Parkinsonism: Possible disease modifying activity. J. Biomed. Mater. Res. A 103(5), 1713-1720.

Reese, C.E., Mikhonin, A.V., Kamenjicki, M., Tikhonov, A., Asher, S.A., 2004. Nanogel nanosecond photonic crystal optical switching. J. Am. Chem. Soc. 126(5), 1493-1496.

Resmini, M., Flavin, K., Carboni, D., 2012. Microgels and nanogels with catalytic activity. Top. Curr. Chem. 325, 307-342.

Rosiak, J., Olejniczak, J., Pękala, W., 1990. Fast reaction of irradiated polymers—I. Crosslinking and degradation of polyvinylpyrrolidone. Int. J. Radiat. Appl. Instrum. C. Radiat. Phys Chem; 36, 747-755.

Rosiak, J.M., Janik, I., Kadlubowski, S., Kozicki, M., Kujawa, P., Stasica, P., et al., 2002. Radiation formation of hydrogels for biomedical application. In Radiation synthesis and modification of polymers for biomedical applications. Final results of a IAEA co-ordinated research project; 1996-2000.

Sabatino, M.A., Bulone, D., Veres, M., Spinella, A., Spadaro, G., Dispenza, C., 2013. Structure of e-beam sculptured poly(N-vinylpyrrolidone) networks across different length-scales, from macro to nano. Polymer 54(1), 54–64.

Sáez-Martínez, V., Olalde, B., Juan, M.J., Jurado, M.J., Garagorri, N., Obieta, I., 2010. Novel bioactive scaffolds incorporating nanogels as potential drug eluting devices. J. Nanosci. Nanotechnol. 10, 2826-2832.

Sakurada, I., Ikada, Y., 1963. Effects of gamma radiation on polymer in solution. IV. Crosslinking and degradation of poly(acrylic acid) in aqueous solution. Bull. Inst. Chem. Res. Kyoto Univ. 41(1), 103-113.

Schmidt, T, Janik, I, Kadlubowski, S, Ulanski, P, Rosiak, JM, Reichelt, R, et al., 2005. Pulsed electron beam irradiation of dilute aqueous poly(vinyl methyl ether) solutions. Polymer 46(23), 9908–9918.

Soni, K.S., Desale, S.S., Bronich, T.K., 2016. Nanogels: An overview of properties, biomedical applications and obstacles to clinical translation. J. Control. Release 240, 109–126.

Spinks, J.W.T., Woods, R.J., 1990. An introduction to radiation chemistry, third ed. John Wiley and Sons Inc., NY. Chapter 7, p. 260 and 285.

Taniguchi, H., 1970. Free-Radical Intermediates in the Reaction of the Hydroxyl Radical with Nitrogen Heterocyclic Compounds. J. Phys. Chem. 74, 3143-3146.

Ulanski, P., Zainuddin, Rosiak, J.M., 1995. Pulse-radiolysis of poly(ethylene oxide) in aqueous-solution. II. Decay of macroradicals. Radiat. Phys. Chem. 46(4-6), 917-920.

Ulanski, P., Janik, I., Rosiak, J.M., 1998. Radiation formation of polymeric nanogels. Radiat. Phys. Chem. 52, 289–294.

Ulanski, P., Rosiak, J.M., 1999. The use of radiation technique in the synthesis of polymeric nanogels. Nucl. Instrum. Methods Phy. Res. Sect. B 151(1–4), 356–360.

Ulanski, P., Kadlubowski, S., Rosiak, J.M., 2002. Synthesis of poly(acrylic acid) nanogels by preparative pulse radiolysis. Radiat. Phys. Chem. 63(3–6), 533–537.

Wu, W., Zhou, S., 2010. Hybrid micro-/nanogels for optical sensing and intracellular imaging. Nano Rev. 1, 5730-5747.